# Micro-scale variations of iron isotopes in fossilized microorganisms

## Magnus Ivarsson[1], Seppo Gehör[2] and Nils G. Holm[1]

[1]*Department of Geology and Geochemistry, Stockholm University, Sweden*
[2]*Department of Geology, University of Oulu, Finland*
*e-mail: magnus.ivarsson@geo.su.se*

**Abstract**: Laser-ablation inductively coupled plasma mass spectroscopy analyses have been performed on carbonaceous filamentous structures that have been interpreted as fossilized microorganisms containing $\sim$10–50 wt % Fe and on non-carbonaceous filamentous structures that have been interpreted to have been formed abiotically containing $\sim$80 wt % Fe. The obtained laser-ablation profiles of the two structural types show a distinct difference in the iron isotopic variations. The centers of the carbonaceous filaments are enriched in $^{57}$Fe and $^{58}$Fe and depleted in $^{56}$Fe. The surficial parts of the filaments display an opposite behavior of the iron isotopes and are thus enriched in $^{56}$Fe and depleted in $^{57}$Fe and $^{58}$Fe. $^{54}$Fe usually follows $^{57}$Fe and $^{58}$Fe but in some cases it follows $^{56}$Fe instead. The outer, surficial parts enriched in $^{56}$Fe have been interpreted as iron oxides precipitated on the surfaces of the microorganisms as they mediate oxidation of the iron to achieve metabolic energy. The laser-ablation profiles of the abiotically formed non-carbonaceous filamentous structures do not show the same characteristics as the carbonaceous filaments but only irregular elevations of $^{56}$Fe. The characteristic profile patterns of the isotope variations in the microfossils suggest that microbially formed iron oxides may be enriched in $^{56}$Fe. If that is the case the isotopic profiles could be used to distinguish abiotically formed iron oxides from biologically formed oxides.

## Introduction

The deep biosphere, found at hydrothermal vent areas on the ocean floors, has been recognized to consist mainly of chemoautotrophic microorganisms (Staudigel *et al.* 2004; Edwards *et al.* 2005). Such organisms use chemical energy stored in minerals or in compounds dissolved in the hydrothermal fluids as an energy source. The most accessible elements and compounds for such organisms in hydrothermal settings are $H_2$, $H_2S$, S, CO, $CH_4$, $Mn^{2+}$ and $Fe^{2+}$, and electron acceptors could be $CO_2$, $SO_4^{2-}$ or $O_2$. At many hydrothermal vent areas iron oxidizing microorganisms appear to play an important role (Boyd & Scott 2001; Emerson & Moyer 2002; Edwards *et al.* 2003, 2004). Iron oxidizing microorganisms mediate the oxidation of dissolved Fe(II) to ferric oxide/hydroxides Fe(III). Such microorganisms occupy habitats at the interface between two environments with divergent redox chemistry. In contact with oxidized seawater, Fe(II) is out of chemical equilibrium, and redox reactions exploitable by microorganisms can occur. The reactions are relatively slow, and the microorganisms can catalyse the reactions and gain metabolic energy in the process.

Recent observations of encrusted and fossilized microorganisms in drilled samples from sub-seafloor environments indicate that iron is probably the dominating energy source for microbes in such environments as well (Thorseth *et al.* 1995, 2001, 2003; Ivarsson *et al.* 2008). High contents of iron, iron encrusted cells and association with minerals and materials that contain reduced iron suggest that iron is a crucial element in sub-seafloor environments. Unweathered basalt minerals such as olivine and pyroxene contain high amounts of reduced iron that microbes can scavenge. Volcanic glass is another material that microorganisms have been observed attached to and boring into, and which contain high amounts of reduced iron. So-called tunnel structures or galleries that are a result of microbial activity have during the last ten years been recognized as a widely spread phenomenon in the world's ocean floors, both in modern and in ancient ones (Giovannoni 1996; Furnes *et al.* 1996; Fisk *et al.* 1998; Furnes & Staudigel 1999; Furnes *et al.* 2001; Fisk *et al.* 2003; Furnes *et al.* 2004; Staudigel *et al.* 2004).

During the last decade an increased amount of research regarding the role of iron in biogeochemical cycles has been carried out, generally with a focus on iron isotopes (e.g. Beard & Johnson 2004; Johnson *et al.* 2004; Johnson & Beard 2006). The possibility of biogeochemical fractionation and the use of iron isotopes as 'biosignatures' have been tantalizing both for research connected to environments on our planet as well as a potential way of distinguishing between biological and abiological features in extraterrestrial samples

(Anbar 2004; Anand *et al.* 2006). Although there is no doubt that metabolic processing of Fe produces isotopic fractionation (Beard *et al.* 1999, 2003; Croal *et al.* 2004; Johnson *et al.* 2004), similar Fe isotope fractionations may be produced by abiologic processes (Anbar *et al.* 2000; Bullen *et al.* 2001; Johnson *et al.* 2002; Roe *et al.* 2003; Welch *et al.* 2003; Icopini *et al.* 2004). Thus, it has been questioned whether or not a biosignature based on iron isotopic fractionation can be preserved in the geologic record (Balci *et al.* 2006).

In this study we use laser-ablation inductively coupled plasma mass spectroscopy (ICP-MS) to study variations in iron isotopes on a micro-scale. We have studied carbonaceous filamentous structures previously described by Ivarsson (2006) and Ivarsson *et al.* (2008) and which have been interpreted as fossilized microorganisms. We have also studied non-carbonaceous filamentous structures that we interpret to have formed abiotically, comparing their isotopical composition to the isotopical composition of the microfossils.

The samples used in this study were collected during the Ocean Drilling Program (ODP) Leg 197 at the Emperor Seamounts in the Pacific Ocean. During this leg, three seamounts belonging to the Emperor Seamounts were drilled: Detroit, Nintoku and Koko Seamounts. The collected samples consist of drilled ocean floor basalts from all three seamounts. These basalts are fractured and veined to varying degrees depending on where in the volcanic pile they were collected. The veins are filled with secondary, hydrothermally formed minerals such as calcite, aragonite and gypsum (Tarduno *et al.* 2002). The filamentous structures studied in this work are found in the veins where they are attached to the vein walls and entombed in the vein filling minerals.

## Methods

The samples were prepared as doubly polished thin sections ($\sim$150–200 μm in thickness) due to their advantages in studying microfossils in volcanic rocks (Ivarsson 2006).

Filamentous structures and their association with iron oxide phases were first studied with light optical microscopy, environmental scanning electron microscopy (ESEM) and energy dispersive spectrometry (EDS). The ESEM analyses were performed using a Philips XL 30 ESEM-FEG which is a field emission microscope. EDS analyses were performed using a Philips EDAX (energy dispersive analysis of x-rays) instrument. The samples were subjected to a pressure of 0.5 torr and the accelerating voltage was 20 kV. The EDS analyses were performed by standardless quantification. The point detection of the EDS instrument is in the size range of 1 micrometer (μm). Analyses of microfossils with the EDS is thus very precise and the measurements are not mixed with the surrounding minerals.

As a next step they were analysed with laser-ablation ICP-MS. The laser that was used was a New Wave UP 213 that was connected to a Thermo Elemental X Series ICP-MS. The carrier gas in the laser was argon. Different sizes of the laser beam were used (5–60 μm) depending on the size of the filamentous structures. In general, a thicker beam size gives better results. The filaments do not vary much in thickness ($\sim$2–10 μm) but do so in length ($\sim$10–200 μm). Variations in thickness are usually due to different thicknesses of the deposited iron oxides onto the filaments. The filaments themselves are usually only a couple of micrometres wide. Short filaments are usually more difficult to analyse with a thick beam size compared to long filaments, and thus long filaments were mostly selected for the laser-ablation analyses. Since laser ablation is a destructive method long filaments were also selected because parts of them are still left after the analyses and can be used as a reference material.

Each analysis or run results in a profile through the analysed material. This profile shows a curve for each analysed element or isotope that reflects the occurrence of the element versus time. Depending on which material is analysed, the curves vary with respect to each other. In most profiles certain elements or isotopes are selected over other elements to make the interpretation of the profiles easier. An element like Ca, for example, is usually excluded since it dominates in the calcite and would only make the profiles more difficult to decipher.

The destructiveness of this method means that each run needs to be carefully targeted (beam size, path and length of the run, surrounding phases) and each element or isotope required for the analysis needs to be selected in advance. Only one opportunity is given and the material is relatively limited.

## Results

### Filamentous structures

The filamentous structures found in the samples were divided into two groups according to chemical composition: carbonaceous filamentous structures and non-carbonaceous filamentous structures (Fig. 1). Carbon-rich filaments from these samples have previously been described by Ivarsson *et al.* (2008). The following is a summary of the descriptions of the carbon-rich filaments and the non-carbonaceous filaments.

### Carbonaceous filamentous structures

The carbon-rich filamentous structures are found attached to the vein walls, which consist of volcanic glass or altered basalt, and are embedded in the vein-filling carbonates. Some filament structures are attached with both ends to the vein walls. Usually, the filament structures have a 'worm-like', smoothly curved appearance and are $\sim$10–100 μm long and $\sim$2–10 μm thick.

The filaments were divided into five groups according to morphology: sheaths, segmented filaments, twisted filaments, amorphous filaments and branched filaments (Fig. 2). Sheaths are made up of hollow, tube-like filamentous structures that resemble one thinner tube inserted into a thicker one. This type is typically attached to the vein walls at both ends as opposed to the other classes which are attached only at one end. This is also the most common kind. Segmented filaments resemble the previous type but lack the consistent
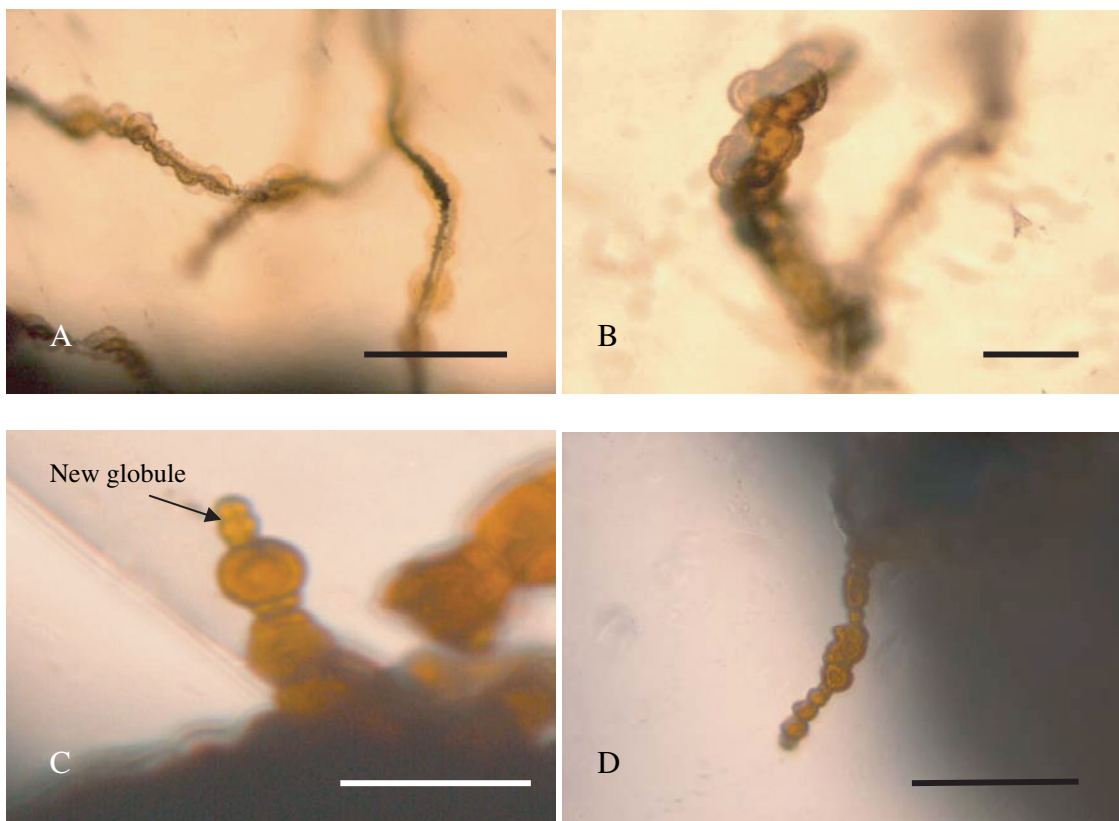
**Fig. 1.** Microphotograph of carbonaceous filamentous structures in A and B. Non-carbonaceous filamentous structures in C and D. Scale bars in A and D: 10 μm, in B and C: 5 μm.

tube shape. Instead, they consist of individual segments making up a long filament. Amorphous filaments are micro-structures with no visual inner texture. The only characteristic feature is a thicker, spherical end at the top of the filament like a bean on a stalk. Twisted filaments are the most uncommon type. They were only seen to occur in one single sample. They resemble the two first types in shape but lack the tube-like outline as well as the segments. Instead, the filaments are twisted in a screw-like fashion. Branched filaments consist of a group of filamentous structures that branch off from each other creating a complicated network. This type is abundant where they occur and occupy much space. In some samples they fill a whole vug or parts of veins. All filament types show a similar range of thicknesses (2–10 μm) except the amorphous filaments that never exceed 2 μm in thickness.

EDS analyses showed that the carbon-rich filaments have an iron content of ~10–50 wt% Fe. The filaments are also closely associated with globular iron oxides both in their close vicinity and deposited onto the surfaces of the filaments. EDS analyses of the iron oxides found in the close vicinity of the filaments show iron contents up to 80 wt% but no carbon content. The iron oxides observed on the fossilized filaments have iron contents similar to the iron contents of the filaments.

The carbon-rich filamentous structures have a carbon content that ranges between ~10 and 50 wt% C (Table 1).

Time-of-flight secondary ion mass spectrometry (ToF-SIMS) analyses showed a concentration of $C_2H_4$, phosphate and lipids to the filamentous structures. Staining with the pigment PI (propidium iodide), which is a dye that binds to dead bacteria cells and remnants of DNA, showed that PI binds to parts of the filaments (Ivarsson *et al.* 2008).

Non-carbonaceous filamentous structures

Non-carbonaceous filamentous structures resemble the carbonaceous filamentous structures morphologically to some extent. They are attached to the vein walls and embedded in carbonates just like the carbonaceous filaments. They are in the same size range as the carbonaceous filaments except in length. Non-carbonaceous filaments seldom exceed 30 μm in length while carbonaceous filaments can reach up to ~100 μm in length. The non-carbonaceous filaments are bright reddish in color and have an undulating appearance that increases as the filament becomes longer. The short filaments are usually straight and have a much stiffer appearance than carbonaceous filaments. The non-carbonaceous filaments appear to have no internal morphology in comparison to the sometimes quite complex internal morphology of the carbonaceous filaments. The greatest difference is the characteristic edifice with globules (~1–2 μm in diameter) connected to each other with short and thin interfaces in between (Fig. 2C). A filament consisting of several globules almost adopts the appearance of a string of pearls (Fig. 2D). At
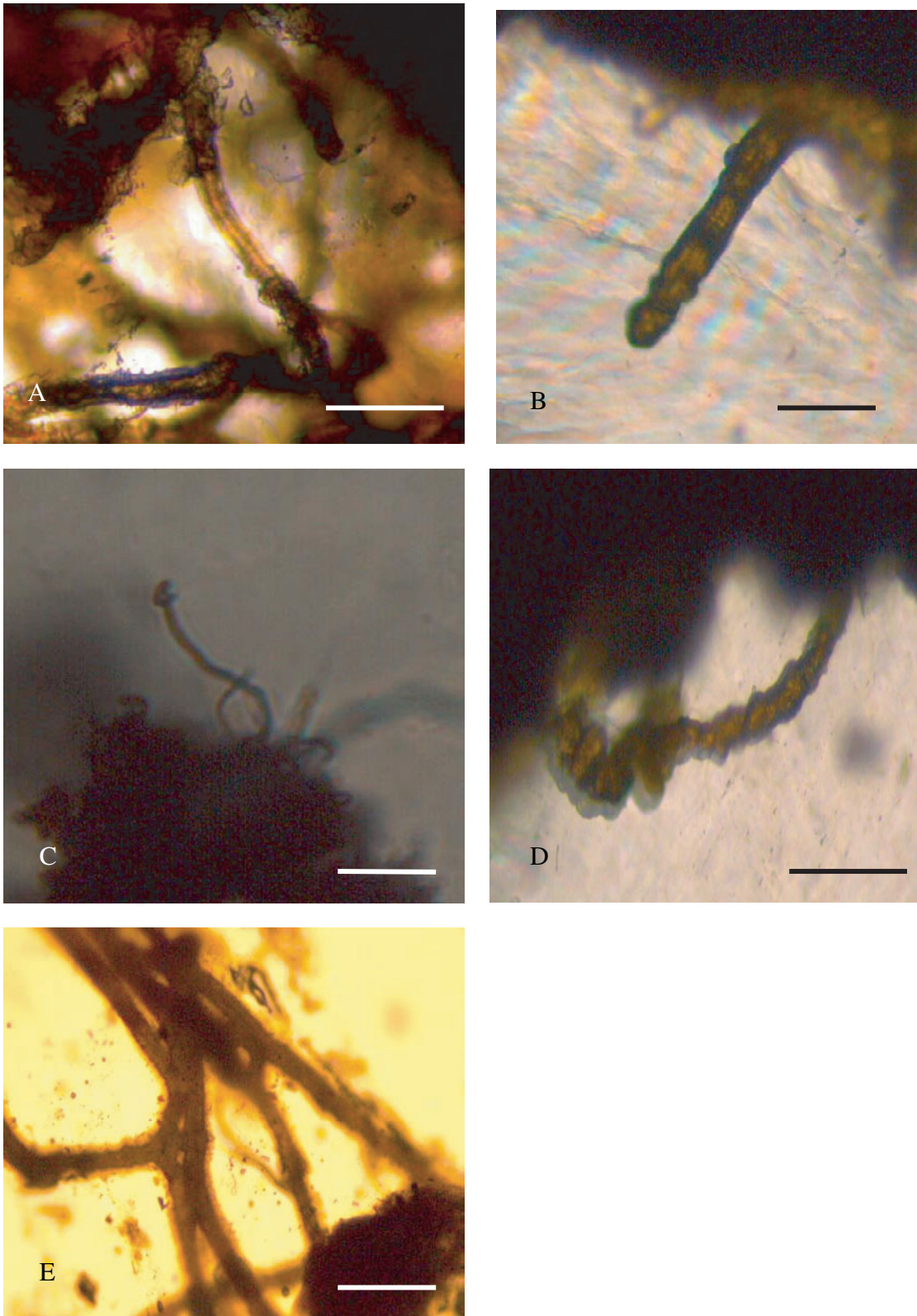
**Fig. 2.** Microphotographs obtained with transmission light microscope showing the different types of fossilized filaments according to morphology. A: sheaths (1206A-18R-1, 104), B: segmented filament (1204B-12R-1, 24), C: amorphous filament (1205A-6R-2, 53), D: twisted filament (1203A-30R-1, 63), E: branched filaments (1203A-57R-3, 40). Scale bars: 5 μm.

Table 1. *Chemical compositions of carbonaceous filamentous structures*

|  | C | O | Na | Mg | Al | Si | Cl | K | Ca | Ti | Fe | Total |
|---|---|---|---|---|---|---|---|---|---|---|---|---|
| 1206A-18R-1, 104 | 50.42 | 18.28 | 0.44 | 3.76 | 5.73 | 16.01 |  | 1.71 | 1.37 |  | 2.28 | 100.00 |
| 1204B-12R-1, 24 | 40.95 | 23.68 | 0.71 | 0.79 | 1.12 | 2.58 | 0.77 |  | 1.39 | 0.69 | 27.32 | 100.00 |
| 1205A-6R-2, 53 | 9.53 | 34.86 |  | 1.44 | 1.84 | 4.45 | 0.54 |  | 1.84 | 1.09 | 44.42 | 100.00 |
| 1203A-30R-1, 63 | 24.70 | 33.60 | 1.03 | 2.37 | 3.74 | 16.75 |  | 2.54 |  |  | 15.28 | 100.00 |
| 1203A-57R-3, 40 | 51.39 | 23.09 |  | 4.74 | 1.72 | 8.32 |  |  | 3.49 |  | 7.26 | 100.00 |

Table 2. *Chemical compositions of non-carbonaceous filamentous structures* (*NCFS*)

|  | $Fe_2O_3$ | $SiO_2$ | MgO | Total |
|---|---|---|---|---|
| **197-1203A-18R-2, 72** |  |  |  |  |
| NCFS1 | 84.32 | 11.22 | 4.46 | 100.00 |
| NCFS2 | 81.61 | 12.66 | 5.72 | 100.00 |
| NCFS3 | 89.58 | 10.42 |  | 100.00 |
| NCFS4 | 91.28 | 8.72 |  | 100.00 |
| NCFS5 | 89.79 | 10.21 |  | 100.00 |
| NCFS6 | 90.41 | 9.59 |  | 100.00 |
| NCFS7 | 88.69 | 11.31 |  | 100.00 |
| NCFS8 | 90.58 | 9.42 |  | 100.00 |
| NCFS9 | 90.54 | 9.46 |  | 100.00 |
| NCFS10 | 90.49 | 9.51 |  | 100.00 |
| NCFS11 | 91.36 | 8.64 |  | 100.00 |
| **197-1203A-65R-3, 40** |  |  |  |  |
| NCFS12 | 93.55 | 6.45 |  | 100.00 |
| NCFS13 | 88.12 | 11.88 |  | 100.00 |
| NCFS14 | 87.08 | 12.92 |  | 100.00 |
| NCFS15 | 92.28 | 7.72 |  | 100.00 |
| NCFS16 | 92.95 | 7.05 |  | 100.00 |
| NCFS17 | 93.73 | 6.27 |  | 100.00 |
| NCFS18 | 92.09 | 7.91 |  | 100.00 |
| NCFS19 | 92.30 | 7.70 |  | 100.00 |
| NCFS20 | 93.05 | 6.95 |  | 100.00 |
| NCFS21 | 91.53 | 8.47 |  | 100.00 |

the end of a filament it is possible to view the filament-like interface that connects two globules as well as an indication of a new globule yet to become whole (Fig. 2C).

Globular iron oxides ($\sim 1$–2 $\mu$m in diameter) are found throughout the samples, usually assembled in clusters of several hundred globular iron oxides. These can be found close to both carbonaceous and non-carbonaceous filamentous structures as well as completely non-associated with either one. The globules are seldom mistaken for filamentous structures but the globules that are the building blocks of non-carbonaceous filaments are similar in appearance.

EDS analyses show that the non-carbonaceous filaments almost exclusively contain iron, with an $Fe_2O_3$ content ranging between $\sim 80$ and $\sim 95$ wt% Fe (Table 2). Minor amounts of $SiO_2$ ($\sim 10$ wt%) occur and in some rare cases MgO ($\sim 5$ wt%). These elements are probably a result of the mixing of surrounding phases such as calcite and basalt as well as minor incorporations of such elements from the phases mentioned during the formation of the filaments. No carbon is detected in the filaments and the dye PI is not binding to them.

*Appearance of laser-ablation profiles*

Around 50 filaments were analysed with laser ablation. Some filaments that were over 100 $\mu$m in length were analysed more than once to observe potential differences or to confirm earlier measurements in the same filaments. In some cases the angle of entrance into the filament was not completely straight but oblique to achieve a longer run within the filament and a more accurate analysis.

All profiles were started and stopped in the vein mineral that the fossilized filaments are embedded in, at a distance from both the filament and the basalt which is a guarantee of no contamination. In the middle of the run the filaments are entered and after some time, depending on how thick the filaments are and the beam size that is used, the filaments are left and vein minerals are entered once again. The profiles have a relatively mutual and characteristic appearance. In the beginning and at the end when the beam is in the vein minerals, the curves are relatively flat with no distinctive features. Peaks or dips occur sporadically due to homogeneities in the calcite composition and minor inclusions of various phases. Calcite and aragonite contain many iron oxides/oxyhydroxides, manganese oxides or parts of altered basalt/volcanic glass/palagonite. Such occurrences of various phases result in local anomalies, but otherwise vein minerals are characterized by high calcium peaks.

As soon as the filaments are entered most elements decrease and iron increases. In some filaments elements such as Mn, Mg and S sometimes follow Fe and increase in comparison to the other elements, but usually only iron increases. This increase of iron in the filaments results in a characteristic bump in the middle of all the filament profiles (Fig. 3).

In several cases there is a dip in the iron curves in the middle of the filaments which results in a twin iron peak in the filaments. In between these dips the elements of the vein minerals increase. These dips probably reflect the inner morphology of some of the filaments that are tubular and hollow inside.

*Elements*

The focus of the analyses was to study differences in iron isotopes but some elements were also analysed contemporaneously to detect correlations or variations between some elements. The elements that were analysed were Fe, Mn, Mg, S, P and Ca. The most obvious correlation is between Mn and Fe, for usually the heavier Fe isotopes. There is also a correlation between Mg and Fe as well as S and Fe. However,

Fig. 3. (*cont.*)
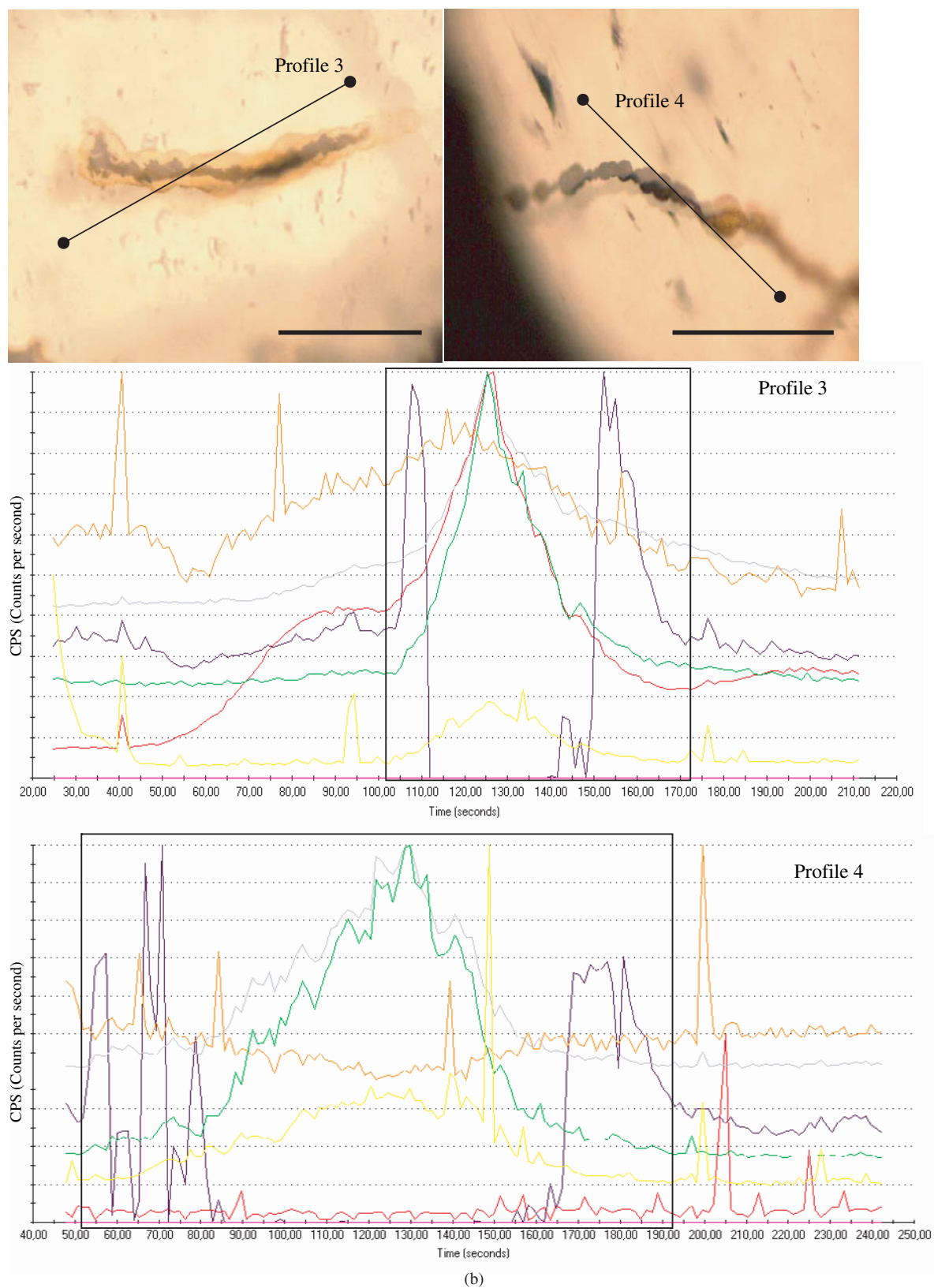
**Fig. 3.** Laser-ablation profiles in carbonaceous filamentous structures. Microphotographs obtained with a light transmission microscope. Rectangle areas show the profile of the filamentous structure. Scale bars: 10 μm except profile 3:5 μm.

| Key | Symbol | Mass |
|---|---|---|
| | 54Fe | 53,94 |
| | 56Fe | 55,94 |
| | 57Fe | 56,94 |
| | 34S | 33,97 |
| | 58Fe | 57,93 |
| | 40Ca | 39,96 |
| | 24Mg | 23,98 |
| | 55Mn | 54,94 |
| | 31P | 30,97 |

(a)
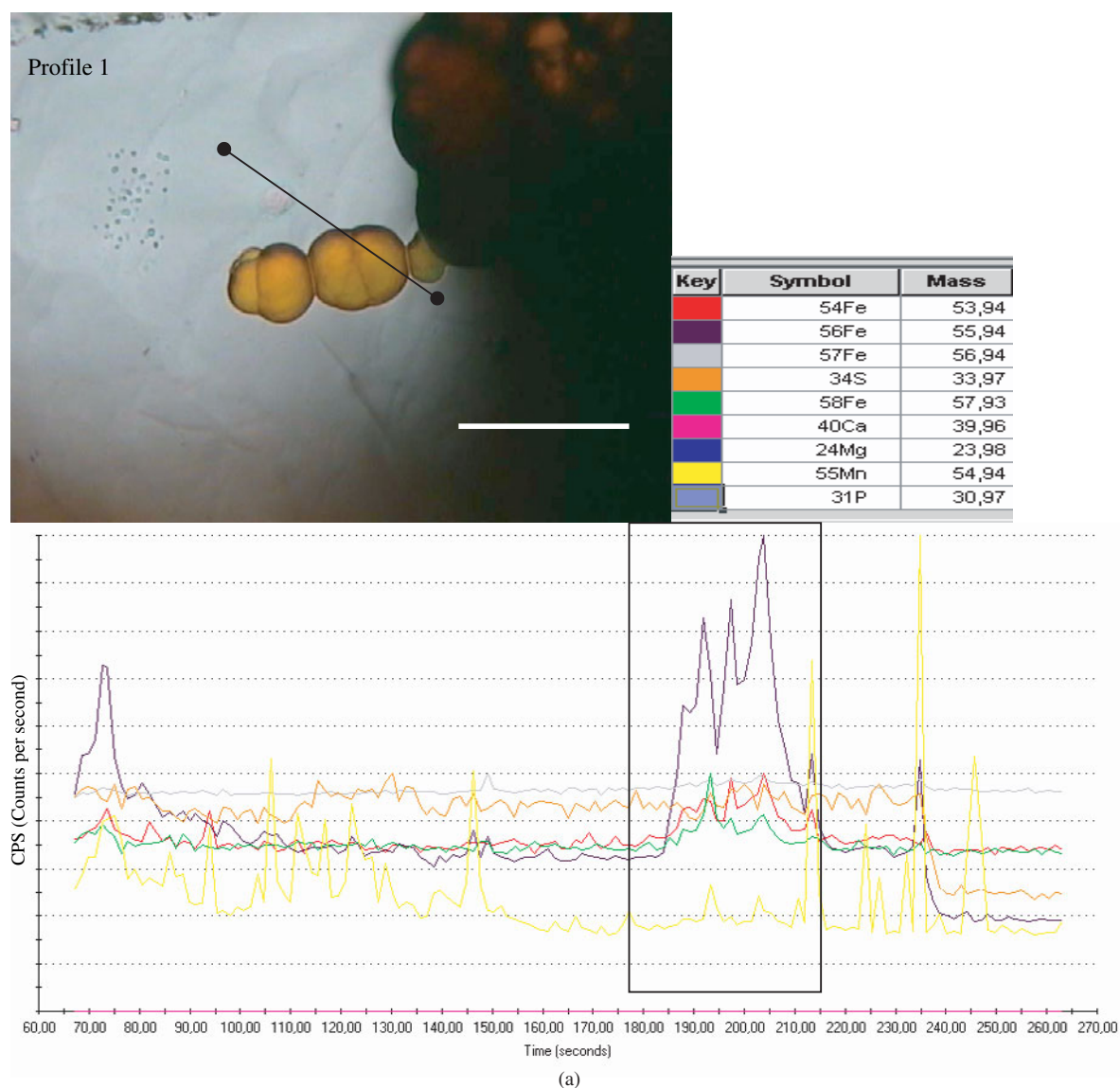
**Fig. 4.** (*cont.*)

these correlations are occasional, and S in particular sometimes shows the opposite behavior. In some samples P and S correspond with each other and have a mutual opposite relationship with Fe in the filaments. In such cases P and S are depleted in the filaments while Fe is enriched. However, when S correlates with Fe in the filaments both S and Fe are enriched.

*Fe isotopes in carbonaceous filamentous structures*

The iron isotopes follow a characteristic trend throughout the analyses of the filaments (Fig. 3). The heavier iron isotopes, $^{57}$Fe and $^{58}$Fe, are exclusively enriched in the interior of the filaments and $^{56}$Fe is depleted. $^{54}$Fe usually follows the trend of the heavier isotopes and is enriched in the filaments but in some cases it is depleted. $^{56}$Fe, on the other hand, is almost always enriched in the outer layers of iron oxides that are precipitated or deposited onto the fossilized filaments. These outer zones of the filaments are also always characterized by

the lack of $^{57}$Fe and $^{58}$Fe. In the cases when $^{54}$Fe is depleted from the interior of the filaments it sometimes follows the trend of $^{56}$Fe and is enriched in the outer iron oxides, but usually it is totally missing. Thus, the characteristic profile of a fossilized filament is a peak of $^{56}$Fe at the entrance of the filament. This peak is followed by a dip of $^{56}$Fe and a major peak of $^{57}$Fe, $^{58}$Fe and usually also $^{54}$Fe. This peak that represents the interior of the filaments is in most cases characterized by a small dip in the middle due to the hollow structure of the filaments. The profile ends with a decrease in $^{57}$Fe, $^{58}$Fe and $^{54}$Fe and a peak in $^{56}$Fe due to entrance into the outer iron oxides. When the beam exits the filaments, there is a decrease in all iron peaks and the peaks of the host mineral increase.

*Fe isotopes in non-carbonaceous filaments and host rock*

The laser-ablation profiles of the non-carbonaceous filamentous structures differ considerably to the profiles of
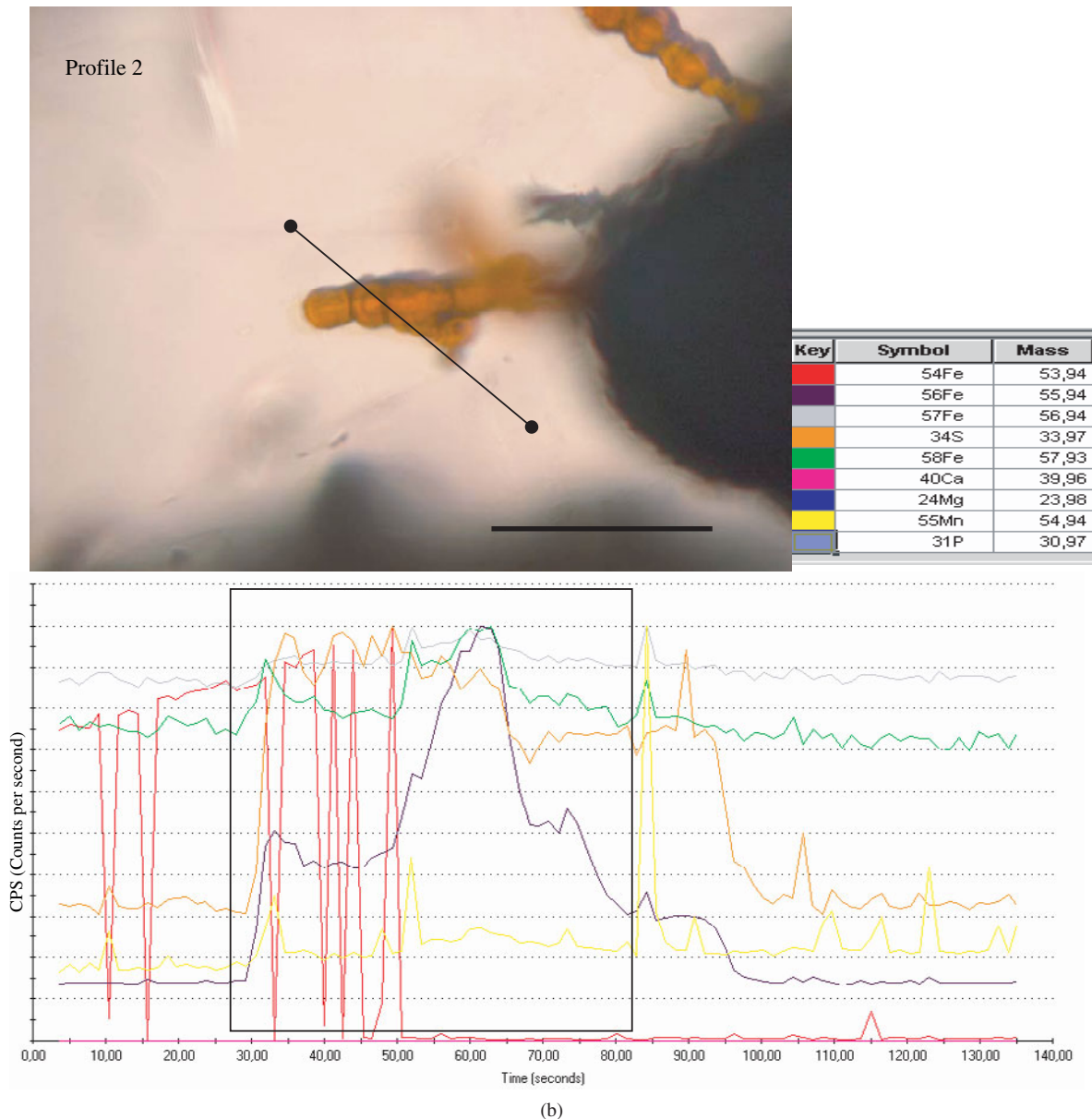
Fig. 4. Laser-ablation profiles in non-carbonaceous filamentous structures. Rectangle areas show the profile of the filamentous structure. Scale bars in profile 1: 5 μm and in profile 2: 10 μm.

carbonaceous filaments (Fig. 4). The enrichment of $^{56}$Fe in the outer layers and depletion in the interiors as well as the reverse behaviour of $^{57}$Fe, $^{58}$Fe and to some extent $^{54}$Fe is not seen in non-carbonaceous filaments. Instead, the profiles of non-carbonaceous filaments show one major peak in which $^{56}$Fe, above all, is enriched. The other iron isotopes show slight enhancements. $^{54}$Fe is the isotope that follows $^{56}$Fe the most. $^{58}$Fe and in particular $^{57}$Fe show only minor changes. The $^{57}$Fe profile is sometimes completely unaffected when a non-carbonaceous filament is entered.

Laser-ablation profiles that start in the calcite and then enter the host rock show a similar trend as the non-carbonaceous filaments with enhanced $^{56}$Fe and $^{54}$Fe values (Fig. 5). $^{57}$Fe and $^{58}$Fe show less enhancements and $^{57}$Fe is sometimes

unaffected. The profiles of the basalts also show much stronger irregularities due to mineral grains or alteration zones at the vein boundaries.

## Discussion

### Origin of the carbonaceous filamentous structures

The carbon content, the detection of $C_2H_4$, phosphates and lipids with the ToF-SIMS as well as the binding of PI led Ivarsson *et al.* (2008) to suggest a biogenic origin for the carbonaceous filaments. Close morphological resemblance to contemporaneous microorganisms and other fossilized microorganisms further support that interpretation.
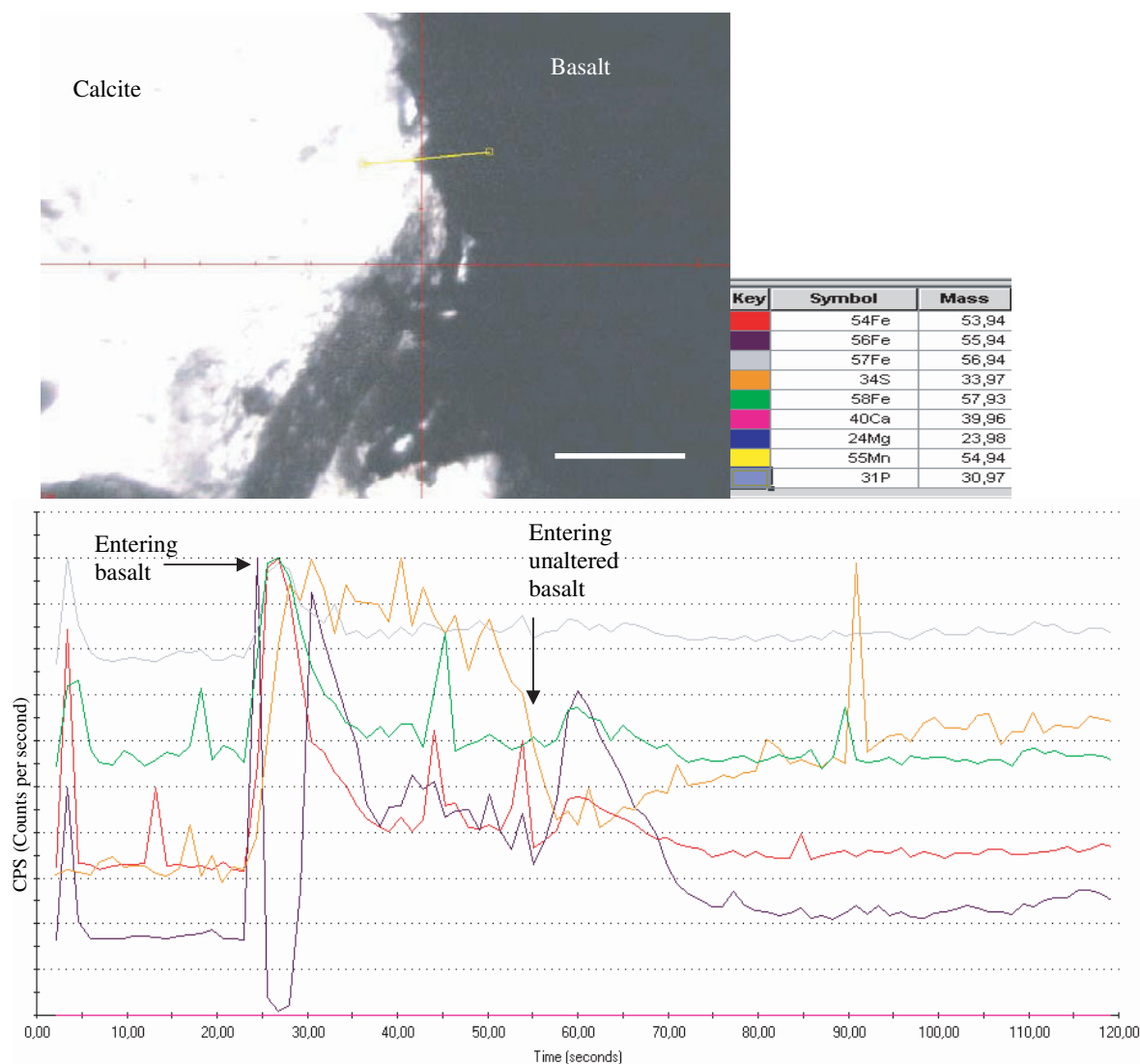
**Fig. 5.** Video microscope image and related laser-ablation profile showing the variation of iron isotopes in basalt. Scale bar: 100 μm.

The microorganisms were interpreted to have lived in the veins as long as fluids were circulating in them (Ivarsson *et al.* 2008). As soon as the carbonates were precipitated and the veins were filled, the fluid circulation ended and the microorganisms died and were trapped within the mineral phases. Considering the high grade of preservation, the mineral formation process was probably a relatively quick event.

Several circumstances concerning the appearance of the filaments point in the direction of microbial involvement in iron oxidation. The high carbon content, the close association with iron oxides and the deposition of iron oxides on the surfaces of the filaments suggest involvement in iron oxidation. Thorseth *et al.* (1995, 2001, 2003) made similar interpretations and suggested that iron-rich encrustations on the cells were a result of microbial iron oxidation to gain metabolic energy. Furthermore, cell-like globules that were interpreted as fossilized cells and found in cavities in zeolites in our samples have acted as nuclei for iron

precipitation and formation of goethite and hematite (Ivarsson *et al.* 2008).

According to Ghiorse (1984), iron oxidizing bacteria produce unique morphological structures such as sheaths and stalks that characterize this group of microbes. Features like attachment to a solid, a bean-shaped cell at the top of a stalk and a twisted stalk structure are all characteristics of *Gallionella* spp (Ehrlich 1996). Furthermore, the tubular-like sheath textures resemble the bacterial sheaths described by Emerson & Moyer (2002) from samples taken at Loihi Seamount. Emerson & Moyer (2002) interpreted them as encrusted sheaths of iron oxidizing *Leptothrix ochracea*. In some samples the filaments are covered by globular iron oxides as if they were deposited on the fossilized bacteria. According to Ghiorse (1984) sheathed bacteria are more likely to be iron-depositing than iron-oxidizing, meaning that they bind preoxidized iron at their cell surface. Transitions between being iron oxidizing and iron depositing behaviour

are common among several iron bacteria, and it is usual that iron oxidizing bacteria deposit the oxidized iron in their sheaths and stalks (Ehrlich 1996).

Hydrothermal fluids often contain high amounts of $Fe^{2+}$, at least acidic hydrothermal solutions, which the microorganisms can scavenge and oxidize to $Fe^{3+}$. Another source of reduced iron is the basalts. Unweathered basalt minerals such as olivine and pyroxene as well as volcanic glass contain $Fe^{2+}$ which the microorganisms can use as an energy source. Rogers & Bennet (2004) showed that microorganisms preferentially colonize and weather silicates that contain the limiting nutrients Fe and P, while leaving similar non-nutrient silicates uncolonized and unweathered. It is a well-known fact nowadays that iron oxidation microorganisms live around hydrothermal vents on the ocean floors where they scavenge ferrous iron from the hydrothermal fluids, and a similar mode of life cannot be excluded for sub-seafloor microorganisms (Boyd & Scott 2001; Emerson & Moyer 2002; Edwards *et al.* 2003, 2004, 2005).

### Origin of the non-carbonaceous filamentous structures

The lack of carbon, biomarkers and the inability to bind to PI indicates that the non-carbonaceous filamentous structures are not biogenic in origin. Their chemical composition, dominated by mainly iron and oxygen, is concordant with ordinary iron oxides, and their close morphological resemblance with the globular iron oxides found throughout the samples supports an abiotic origin. However, the fact that they occur as filamentous structures and not assembles in clusters like ordinary iron oxides suggests that their formation is different relative to other iron oxides. Their close morphological resemblance to biogenic filamentous structures is also a reason why their origin as well as their internal structure and morphology are of interest. The ability to distinguish between biogenic and abiogenic filamentous structures is a primary target in research areas such as the sub-seafloor biosphere, the search for the earliest life on Earth as well as the search for an extraterrestrial fossil record (Schopf 1993; Farmer & Des Marais 1999; Gibson *et al.* 2001; Brasier *et al.* 2002; Schopf *et al.* 2002; Brasier *et al.* 2005).

One possible origin of the non-carbonaceous filaments is that globular iron oxides have simply attached to each other and formed these long filament-like structures. However, it is more likely that globular iron oxides would form irregular clusters, as elsewhere throughout the samples, than filaments. Besides, the appearance of the globules connected with some sort of interface, as well as the thin, knob-like structure that they end with, suggest that they 'grow' outwards in length. The embryo globule that is seen at the end of a filament in Fig. 2C further supports the suggestion that the globules grow *in situ*. It appears as if the globules are formed sequentially; when one globule is finished a knob is formed at the end, and from that knob a new globule is formed.

Abiotically formed filamentous micro-structures are known to form in volcanic rocks on the seafloor when lava meets cold seawater (Perfit *et al.* 2003). Bubbles of vaporized seawater rise through the base of lava flows and result in the formation of both centimetre-sized drip-like lava stalactites and micrometre-sized filamentous structures similar to the morphology of filamentous microorganisms.

Self-assembled micrometre-sized filaments, so-called biomorphs, have been synthesized in laboratory experiments (Garcia-Ruiz *et al.* 2003; Hyde *et al.* 2004). Such biomorphs display morphologies similar to microbial filaments, and they have been used to argue for an abiotic origin of precambrian microfossils from the Warrawoona Chert in Western Australia, which have been claimed to represent the oldest known microbial life on Earth (Garzia-Ruiz *et al.* 2003). The biomorphs are grown out of silica-carbonate solutions under ambient pressure and temperatures and at pH ranging from 8.5 to 11. Even though biomorphs containing iron have not yet been produced, a similar formation process could have formed the filamentous iron oxides observed in our samples.

### Isotopic variations on a micro-scale

A significant proportion of the Fe isotope literature has focused on the use of Fe isotopes as a biosignature for life. Such a Fe isotope biosignature would require isotopic fractionations that can only be produced by biology. Although there is no question that metabolic processing of Fe produces isotopic fractionation (Beard *et al.* 1999, 2003; Croal *et al.* 2004; Johnson *et al.* 2005), it is also true that similar Fe isotope fractionations may be produced by abiologic processes (Anbar *et al.* 2000; Bullen *et al.* 2001; Johnson *et al.* 2002; Roe *et al.* 2003; Welch *et al.* 2003; Icopini *et al.* 2004). Balci *et al.* (2006) concluded that any characteristic iron isotope fractionation related to microbial oxidation that might constitute a biosignature is likely to be overprinted by rapid isotopic equilibration between $Fe(II)_{aq}$ and $Fe(III)_{aq}$ pools. Thus, it is unlikely that such a biosignature would be expressed in the geologic record.

Iron isotopic ratios are usually expressed as $\Delta^{56}Fe$ which is normally calculated as:

$$\Delta^{56}Fe = \left[ \frac{{}^{56}Fe/{}^{54}Fe_{sample}}{{}^{56}Fe/{}^{54}Fe_{bulk\ earth}} - 1 \right] \times 10^3 \qquad (1)$$

where ${}^{56}Fe/{}^{54}Fe_{bulk\ earth}$ is defined by a wide variety of terrestrial and lunar rocks.

Since our results are described by profiles of isotopic variations rather than $\Delta^{56}Fe$ values, we can show isotopic trends that are not visual in traditional isotopic measurements. Our profiles show isotopic changes on a micro-scale and not the mean value of a sample. Therefore we are able to show isotopic variations within a fossilized filament and not only give a general isotopic value of a rock that is known to contain fossilized filaments. Our results could perhaps give more detailed isotopic information than a $\Delta^{56}Fe$ value and could maybe also indicate something about the formation processes.

Even though the isotope patterns of microfossils in our samples are consistent and differ notably compared to the non-carbonaceous filaments, the results are too preliminary to be used as a biosignature. However, the profile patterns

show a trend that is probably a result of some fractionation process.

Significant Fe isotope variations in nature are generally restricted to low-temperature systems and occur at phase transformations such as the fluid–vapor or fluid–mineral. The oxidation of dissolved Fe(II) to solid Fe(III) is one process when fractionation of the isotopes normally occurs. In many cases the phase transformations and thus the fractionation can occur in several steps, for example

$$Fe(II)aqueous \rightarrow Fe(III)aqueous \rightarrow Fe(III)solid. \qquad (2)$$
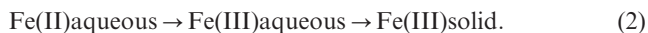
Microorganisms process iron when it is energetically favorable to do so, and where they are able to out-compete abiotic redox reactions. Iron is generally biologically processed in three different ways: (1) lithotrophic or phototrophic metabolism where Fe(II) acts as an electron donor for energy generation and/or carbon fixation; (2) dissimilatory Fe(III) reduction, where Fe(III) acts as an electron acceptor for respiration; and (3) assimilatory Fe metabolism which involves uptake and incorporation into biomolecules. For lithotrophic, phototrophic and dissimilatory Fe metabolism, electron transfer occurs between the cell and Fe that is bound to the cell surface or incorporated in the outer membrane.

The outer layer of the microfossils enriched in Fe is interpreted as iron oxides deposited or precipitated on the surfaces of the filaments by the microorganisms. The iron oxides should thus represent the rest products of the microbial oxidation of iron to achieve metabolic energy. If that is the case, microbially precipitated iron oxides are enriched in lighter iron isotopes, especially $^{56}Fe$, and depleted in heavier iron isotopes. The opposite appears to be the case for the microorganisms themselves which are enriched in heavy iron isotopes and depleted in light iron isotopes. It has been shown previously that ferric hydroxides produced by Fe(II) oxidation under anaerobic conditions have high $\delta^{56}Fe$ values relative to the Fe(II)aq sources (Croal *et al.* 2004). Iron reducing bacteria, on the other hand, are known to produce ferric oxides that contain heavy iron isotopes compared to the iron released to solution that is enriched in $^{56}Fe$ (Brantley *et al.* 2004).

It is difficult to establish the underlying processes for the behavior of iron in the microfossils but two major outlines seem possible: (1) isotopically heavy iron is taken up by the microorganisms and assimilated in their cells which creates a pool of $^{56}Fe$ that will precipitate as ferric oxides; and (2) both heavy and light iron is taken up by the microorganisms but only $^{56}Fe$ is processed by the microorganisms and precipitated as ferric oxides in a later stage. The $^{56}Fe$ is either enzymatically or non-enzymatically processed. The latter may involve the ligand destruction of iron chelates (Ehrlich 1996).

### *Implications*

Our results show a characteristic pattern of the isotopic variations of microfossils that may be used to distinguish between biogenic structures and abiogenic structures. The results further suggest that microorganisms produce ferric

iron oxides enriched in $^{56}Fe$ and depleted in $^{57}Fe$ and $^{58}Fe$. However, to simply use the enrichment of $^{56}Fe$ in iron oxides as a sign of biological activity can be misleading, since the non-carbonaceous filaments are enriched in $^{56}Fe$ as well. It is crucial to recognize the characteristic isotopic pattern, and thus we conclude that a micro-scale study of the isotopic variations is required to distinguish between biologically and abiologically formed $^{56}Fe$ precipitates. However, it is too early to use this method alone to establish biogenicity. Micro-scale studies of iron isotopes should be used as a complement to other methods in an attempt to establish biogenicity of putative microfossils.

### Conclusions

Carbonaceous filamentous structures that are interpreted as fossilized microorganisms and non-carbonaceous filamentous structures that are interpreted to have formed abiotically are observed in samples of volcanic rock drilled at the Emperor Seamounts in the Pacific Ocean. Both groups of filamentous structures are found to be attached to vein walls in fractured basalts and entombed in vein filling carbonates. The similar morphological appearance and the similar occurrence in the rocks show that there is a need to distinguish the two groups from each other, in an attempt to establish biogenicity.

Laser-ablation ICP-MS analysis of the various filamentous structures shows characteristic profile patterns in iron isotopes that differ between the two groups. The centers of the carbonaceous filaments are enriched in $^{57}Fe$ and $^{58}Fe$ and depleted in $^{56}Fe$. The surficial parts of the filaments display an opposite behavior of the iron isotopes and are thus enriched in $^{56}Fe$ and depleted in $^{57}Fe$ and $^{58}Fe$. $^{54}Fe$ usually follows $^{57}Fe$ and $^{58}Fe$, but in some cases it follows $^{56}Fe$ instead. The outer, surficial parts enriched in $^{56}Fe$ have been interpreted as iron oxides precipitated on the surfaces of the microorganisms as they mediate oxidation of the iron to achieve metabolic energy. This may suggest that microbially formed iron oxides are enriched in $^{56}Fe$. The laser-ablation profiles of the abiotically formed non-carbonaceous filamentous structures do not show the same characteristics as the carbonaceous filaments but only irregular elevations of $^{56}Fe$.

It is too early to suggest that the characteristic laser-ablation profiles of the microfossils could be used as a biosignature, but we do conclude that micro-scale studies of iron oxides may resolve some obstacles in attempts to distinguish biologically formed iron oxides from those that are abiologically formed.

### References

Anand, M., Russell, S.S., Blackhurst, R.L. & Grady, M.M. (2006). Searching for signatures of life on mars: an Fe-isotope perspective. *Philos. Trans.* **361**, 1715–1720.

Anbar, A.D. (2004). Iron stable isotopes: beyond biosignatures. *Earth Planet. Sci. Lett.* **217**, 223–236.

Anbar, A.D., Roe, J.D., Barling, J. & Nealson, K.H. (2000). Nonbiological fractionation of iron isotopes. *Science* **288**, 126–128.

Balci, N., Bullen, T.D., Witte-Lien, K., Shanks, W.C., Motelica, M. & Mandernack, K.W. (2006). Iron isotope fractionation during microbially stimulated Fe(II) oxidation and Fe(III) precipitation. *Geochim. Cosmochim. Acta* **70**, 622–639.

Beard, B.L. & Johnson, C.M. (2004). Fe isotope variations in the modern and ancient Earth and other planetary bodies. In *Geochemistry of Non-traditional Stable Isotopes* (*Reviews in Mineralogy and Geochemistry*, vol. 55), eds Johnson, C.M., Beard, B.L. & Albarède, F., pp. 319–357. Mineralogical Society of America.

Beard, B.L., Johnson, C.M., Cox, L., Sun, H., Nealson, K.H. & Aguilar, C. (1999). Iron isotope biosignatures. *Science* **285**, 1889–1892.

Beard, B.L., Johnson, C.M., Skulan, J.L., Nealson, K.H., Cox, L. & Sun, H. (2003). Application of Fe isotopes to tracing the geochemical and biological cycling of Fe. *Chem. Geol.* **195**, 87–117.

Boyd, T.D. and Scott, S.D. (2001). Microbial and hydrothermal aspects of ferric oxyhydroxides and ferrosic hydroxides: the example of Franklin Seamount, Western Woodlark Basin, Papua New Guinea. *Geochem. Trans.* **2**, 45.

Brantley, S.L., Liermann, L.J., Guynn, R.L., Anbar, A., Icopini, G.A. & Barling, J. (2004). Fe isotopic fractionation during mineral dissolution with and without bacteria. *Geochim. Cosmochim. Acta* **68**, 3189–3204.

Brasier, M.D., Green, O.R., Jephcoat, A.P., Kleppe, A.K., Van Kranendonk, M.J., Lindsay, J.F., Steele, A. & Grassineau, N.V. (2002). Questioning the evidence for Earth's oldest fossils. *Nature* **416**, 76–81.

Brasier, M.D., Green, O.R., Lindsay, J.F., McLoughlin, N., Steele, A. & Stoakes, C. (2005). Critical testing of Earth's oldest putative fossil assemblage from the ∼3.5 Ga Apex chert, Chinaman Creek, Western Australia. *Precambr. Res.* **140**, 55–102.

Bullen, T.D., White, A.F., Childs, C.W., Vivit, D.V. & Schultz, M.S. (2001). Demonstration of significant abiotic iron isotope fractionation in nature. *Geology* **29**, 699–702.

Croal, L.R., Johnson, C.M., Beard, B.L. & Newman, D.K. (2004). Iron isotope fractionation by anoxygenic Fe(II)-phototrophic bacteria. *Geochim. Cosmochim. Acta* **68**, 1227–1242.

Edwards, K.J., Bach, W. & McCollom, T.M. (2005). Geomicrobiology in oceanography: microbe-mineral interactions at and below the seafloor. *Trends Microbiol.* **13**, 449–456.

Edwards, K.J., Bach, W., McCollom, T. & Rogers, D.R. (2004). Neutrophilic iron-oxidizing bacteria in the ocean: Their habitats, diversity, and roles in mineral deposition, rock alteration, and biomass production in the deep-sea. *J. Geomicrobiol.* **21**, 393–404.

Edwards, K.J., Rogers, D.R., Wirsen, C.O. & McCollom, T.M. (2003). Isolation and characterization of novel psychrophilic, neutrophilic, Fe-oxidizing, chemolithoautotrophic α- and γ-*Proteobacteria* from the deep sea. *Appl. Environ. Microbiol.* **69**, 2906–2913.

Ehrlich, H.L. (1996). *Geomicrobiology*, 3rd edn, revised and expanded. Dekker, New York.

Emerson, D. & Moyer, C.L. (2002). Neutrophilic Fe-oxidizing bacteria are abundant at the Loihi Seamount hydrothermal vents and play a major role in Fe oxide deposition. *Appl. Environ. Microbiol.* **68**, 3085–3093.

Farmer, J.D. & Des Marais, D.J. (1999). Exploring for a record of ancient Martian life. *J. Geophys. Res.* **104**, 26 977–26 995.

Fisk, M.R., Giovannoni, S.J. & Thorseth, I.H. (1998). Alteration of oceanic volcanic glass: Textural evidence of microbial activity. *Science* **281**, 978–980.

Fisk, M.R., Storrie-Lombardi, M.C., Douglas, S., Popa, R., McDonald, G. & Di Meo-Savoie, C. (2003). Evidence of biological activity in Hawaiian subsurface basalts. *Geochem. Geophys. Geosyst.* **4**, 1103, doi:10.1029/2002GC000387.

Furnes, H. & Staudigel, H. (1999). Biological mediation in ocean crust alteration: how deep is the deep biosphere? *Earth Planet. Sci. Lett.* **166**, 97–103.

Furnes, H., Banerjee, N.R., Muehlenbachs, K., Staudigel, H. & de Wit, M. (2004). Early life recorded in Archean pillow lavas. *Science* **304**, 578–581.

Furnes, H., Muehlenbachs, K., Tumyr, O., Torsvik, T. & Xenophontos, C. (2001). Biogenic alteration of volcanic glass from the Trodos ophiolite, Cyprus. *J. Geol. Soc. Lond.* **158**, 75–84.

Furnes, H., Thorseth, I.H., Tumyr, O., Torsvik, T. & Fisk, M.R. (1996). Microbial activity in the alteration of glass from pillow lavas from hole 896A. *Proc. Ocean Drilling Program, Scientific Results* **148**, 191–206.

Garcia-Ruiz, J.M., Hyde, S.T., Carnerup, A.M., Christy, A.G., Van Krankendonk, M.J. & Welham, N.J. (2003). Self-assembled silica-carbonate structures and detection of ancient microfossils. *Science* **302**, 1194–1197.

Ghiorse, W.C. (1984). Biology of iron- and manganese-depositing bacteria. *Annu. Rev. Microbiol.* **38**, 515–550.

Gibson, E.K, McKay, D.S., Thomas-Keprta, K.L., Wentworth, S.J., Westall, F., Steele, A., Romanek, C.S., Bell, M.S. & Toporski, J. (2001). Life on mars: evaluation of the evidence within martian meteorites ALH84001, Nakhla, and Shergotty. *Precambr. Res.* **106**, 15–34.

Giovannoni, S.J., Fisk, M.R., Mullins, T.D. & Furnes, H. (1996). Genetic evidence for endolithic microbial life colonizing basaltic glass-seawater interfaces. *Proc. Ocean Drilling Program, Scientific Results* **148**, 207–214.

Hyde, S.T., Carnerup, A.M., Larsson, A.-K., Christy, A.G. & Garcia-Ruiz, J.M. (2004). Self-assembly of carbonate-silica colloids: Between living and non-living form. *Physica* A **339**, 24–33.

Icopini, G.A., Anbar, A.D., Ruebush, S.S., Tien, M. & Brantley, S.L. (2004). Iron isotope fractionation during microbial reduction of iron: The importance of adsorption. *Geology* **32**, 205–208.

Ivarsson, M. (2006). Advantages of doubly polished thin sections for the study of microfossils in volcanic rock. *Geochem. Trans.* **7**, 5.

Ivarsson, M., Lindblom, S., Broman, S. & Holm, N.G. (2008). Fossilized microorganisms associated with zeolite-carbonate interfaces in sub-seafloor hydrothermal environments. *Geobiology* **6**, 155–170.

Johnson, C.M. & Beard, B.L. (2006). Fe isotopes: An emerging technique for understanding modern and ancient biogeochemical cycles. *GSA TODAY* **16**, 4–10.

Johnson, C.M., Beard, B.L., Roden, E.E., Newman, D.K. & Nealson, K.H. (2004). Isotopic constraints on biogeochemical cycling of Fe. In *Geochemistry of Non-traditional Stable Isotopes* (*Reviews in Mineralogy and Geochemistry*, vol. 55), eds Johnson, C.M., Beard, B.L. & Albarède, F., pp. 359–408. Mineralogical Society of America.

Johnson, C.M., Roden, E.E., Welch, S.A. & Beard, B.L. (2005). Experimental constraints on Fe isotope fractionation during magnetite and Fe carbonate formation coupled to dissimilatory hydrous ferric oxide reduction. *Geochim. Cosmochim. Acta* **69**, 963–993.

Johnson, C.M., Skulan, J.L., Beard, B.L., Sun, H., Nealson, K.H. & Braterman, P.S. (2002). Isotopic fractionation between Fe(III) and Fe(II) in aqueous solutions. *Earth Planet. Sci. Lett.* **195**, 141–153.

Perfit, M.R., Cann, J.R., Fornari, D.J., Engels, J., Smith, D.K., Ridley, W.D. & Edwards, M.H. (2003). Interaction of sea water and lava during submarine eruptions at mid-ocean ridges. *Nature* **426**, 62–65.

Roe, J.E., Anbar, A.D. & Barling, J. (2003). Nonbiological fractionation of Fe isotopes: Evidence of an equilibrium isotope effect. *Chem. Geol.* **195**, 69–85.

Rogers, J.R. & Bennett, P.C. (2004). Mineral stimulation of subsurface microorganisms: Release of limiting nutrients from silicates. *Chem. Geol.* **203**, 91–108.

Schopf, J.W. (1993). Microfossils of the early Archean Apex Chert: new evidence of the antiquity of life. *Science* **260**, 640–646.

Schopf, J.W., Kudryavtsev, A.B., Agresti, D.G., Wdowiak, T.J. & Czaja, A.D. (2002). Laser-Raman imagery of Earth's earliest fossils. *Nature* **416**, 73–76.

Staudigel, H., Tebo, B., Yayanos, A., Furnes, H., Kelley, K., Plank, T. & Muehlenbachs, K. (2004). The oceanic crust as a bioreactor. In

*The Subseafloor Biosphere at Mid-Ocean Ridges* (*Geophysical Monograph*, vol. 144), eds Wilcock, W.S.D., DeLong, E.F., Kelley, D.S., Baross, J.A. & Cary, S.C., pp. 325–341. American Geophysical Union, Washington DC.

Tarduno, J.A., Duncan, R.A. & Scholl, D.W. (2002). Leg 197 summary. *Proc. Ocean Drilling Program, Initial Reports* **197**, 1–92.

Thorseth, I.H., Pedersen, R.B. & Christie D.M. (2003). Microbial alteration of 0-30-Ma seafloor basaltic glasses from the Australian Antarctic Discordance. *Earth Planet. Sci. Lett*. **215**, 237–247.

Thorseth, I.H., Torsvik, T., Furnes, H. & Muehlenbachs, K. (1995). Microbes play an important role in the alteration of oceanic crust. *Chem. Geol*. **126**, 137–146.

Thorseth, I.H., Torsvik, T., Torsvik, V., Daae, F.L., Pedersen, R.B. & Keldysh-98 Scientific Party (2001). Diversity of life in ocean floor basalt. *Earth Planet. Sci. Lett*. **194**, 31–37.

Welch, S.A., Beard, B.L., Johnson, C.M. & Braterman, P.S. (2003). Kinetic and equilibrium Fe isotope fractionation between aqueous Fe(II) and Fe(III). *Geochim. Cosmochim. Acta* **676**, 4231–4250.